



Design and synthesis of potent Gram-negative specific LpxC inhibitors

U. Faruk Mansoor^{a,*}, Dilrukshi Vitharana^a, Panduranga Adulla Reddy^a, Dayna L. Daubaras^b, Paul McNicholas^b, Peter Orth^c, Todd Black^b, M. Arshad Siddiqui^a

^a Department of Chemistry, Merck Research Laboratories, 320 Bent Street, Cambridge, MA 02141, USA

^b Department of Biology, Merck Research Laboratories, 2015 Galloping Hill Road, Kenilworth, NJ 07033, USA

^c Department of Structural Chemistry, Merck Research Laboratories, 2015 Galloping Hill Road, Kenilworth, NJ 07033, USA

ARTICLE INFO

Article history:

Received 28 October 2010

Revised 21 December 2010

Accepted 21 December 2010

Available online 28 December 2010

Keywords:

LpxC

Gram-negative

ABSTRACT

Antibiotic resistant hospital acquired infections are on the rise, creating an urgent need for novel bactericidal drugs. Enzymes involved in lipopolysaccharide (LPS) biosynthesis are attractive antibacterial targets since LPS is the major structural component of the outer membrane of Gram-negative bacteria. Lipid A is an essential hydrophobic anchor of LPS and the first committed step in lipid A biosynthesis is catalyzed by a unique zinc dependent metalloamidase, UDP-3-O-(R-3-hydroxymyristoyl)-N-acetylglucosamine deacetylase (LpxC). LpxC is an attractive Gram-negative only target that has been chemically validated by potent bactericidal hydroxamate inhibitors that work by coordination of the enzyme's catalytic zinc ion. An exploratory chemistry effort focused on expanding the SAR around hydroxamic acid zinc-binding 'warheads' lead to the identification of novel compounds with enzyme potency and antibacterial activity similar to CHIR-090.

© 2010 Elsevier Ltd. All rights reserved.

The growing emergence of multidrug resistant bacteria in hospital and community clinics remains an important public health concern throughout the world.^{1,2} Resistance developed by different Gram-negative bacterial species including strains of *Escherichia coli* and *Pseudomonas aeruginosa* to antibiotics targeting peptidoglycan, DNA replication, or protein biosynthesis³ has driven the search for identification and development of novel antibacterial targets.⁴ The Gram-negative bacterial cell wall is surrounded by an outer membrane comprised of charged lipopolysaccharide (LPS)^{5,6} molecules which serve as a permeability barrier to protect the bacterium against antibiotics.⁷ The hydrophobic anchor of LPS is lipid A, a phosphorylated, B(1,6)-linked glucosamine disaccharide hexaacetylated with N-linked and O-linked fatty acids. Lipid A is essential for bacterial growth and viability, and the inhibition of its biosynthesis is lethal to bacteria.^{8,9} Bacterial strains containing a defect in lipid A biosynthesis are hypersensitive to antibiotics^{10–12} and it is this observation which has led many research groups and organizations to focus on targeting lipid A biosynthesis to develop safe and effective antibacterial agents.^{13–16}

UDP-3-O-(R-3-hydroxymyristoyl)-N-acetylglucosamine deacetylase (LpxC) catalyzes the deacetylation of UDP-3-O-(R-3-hydroxymyristoyl)-N-acetylglucosamine, the first committed step in the biosynthesis of lipid A.^{17–20} LpxC is a zinc-dependent amidase, functioning via a general acid–base catalyst pair mecha-

nism.^{21–23} The X-ray crystal structure of LpxC from *Aquifex aeolicus* (*aaLpxC*) reveals a catalytic zinc ion (Zn_A^{2+}) coordinated by H79, H238, D242, and a solvent molecule at the base of a ~20 Å-deep active site cleft.²⁴ An inhibitory zinc (Zn_B^{2+}) is bound in the presence of excess zinc to residues E78 and H265 and a myristoyl fatty acid which extends out into a hydrophobic tunnel. This tunnel is required for efficient catalysis,^{24,25} as confirmed by NMR and X-ray crystallography studies,^{26,27} accommodating the long fatty acid side chain attached to the N-acetylglucosamine group of the substrate analog inhibitor TU-514.^{28–30}

Inhibitors of LpxC like TU-514 and amphipathic benzoic acid derivatives (**1**)³¹ bind solely to the hydrophobic tunnel showing moderate enzyme inhibitory activity (Fig. 1). However, early work¹³ clearly confirmed that the LpxC inhibitor affinity was significantly improved by the presence of a suitable 'warhead' that completed a square pyramidal zinc coordination polyhedron as well as a pendant 'tail' that bound to the aforementioned hydrophobic tunnel. Optimization resulted in (**2**), a hydroxamic acid attached to a 2-phenyloxazoline ring system. This was a potent inhibitor of *E. coli* LpxC (*eeLpxC*) but showed 50- to 100-fold weaker in vitro activity toward the *P. aeruginosa* LpxC enzyme (*paLpxC*). More recent work by the Chiron Corporation identified compounds containing the hydroxamic acid linked to an aromatic moiety by a peptide linker.¹⁴ This series have K_i values of ~100 nM against the isolated *paLpxC* enzyme and inhibit *E. coli* growth at minimal inhibitory concentrations (MICs) ranging from 1.25 to 12.5 µg/mL.

Here, we report the design and synthesis of novel inhibitors of LpxC. In a previous study targeting novel zinc-binding warheads,

* Corresponding author.

E-mail address: umar.faruk.mansoor@merck.com (U. Faruk Mansoor).

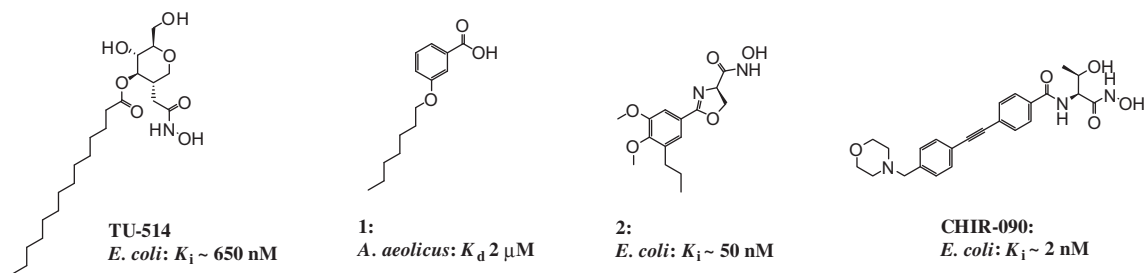


Figure 1. Literature examples of LpxC inhibitors.

we were able to identify linear non-polar groups which made favorable intermolecular interactions within the hydrophobic tunnel of LpxC. When these fragments were combined with the hydroxamic acid zinc binding group by way of a peptide linker, a novel series of potent inhibitors were identified.

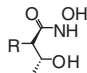
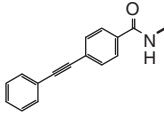
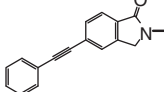
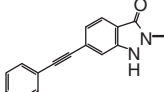
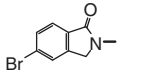
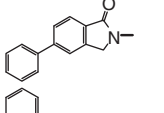
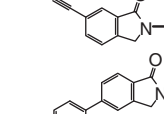
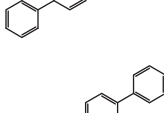
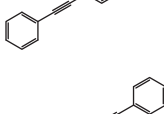
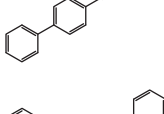
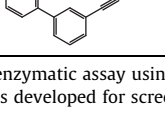
Two separate series of inhibitors were designed and synthesized. Through unpublished in-house X-ray crystallography studies with *aa*LpxC it was known the peptide linker made both polar and non-polar interactions within the enzyme active site with Lys-227 and Phe-180, respectively. Modifications to incorporate the *gem*-dimethyl hydroxyl moiety lead to minor improvements in both biochemical and cellular potency. The two series of inhibitors differed by the fusion of the hydrophobic fragment to this peptide linker. Attaching the peptide linker by cyclizing through the amide NH gave rise to the benzolactam series (Table 1). The synthetic methods used for the preparation of these analogs are illustrated in Scheme 1. Heating *O*-*tert*-butyl-L-threonine *tert*-butyl ester hydrochloride in the presence of methyl 4-bromo-2-(bromo-methyl)benzoate furnished the benzolactam. Sonogashira coupling with various alkynes resulted in extension of the hydrophobic fragments. Acid hydrolysis of the protecting groups and subsequent peptide coupling with TBS-ONH₂ provided the hydroxamic acids after aqueous workup. Unfortunately, capping of the amide NH resulted in the loss of a key hydrogen bonding interaction with Thr-179, with a subsequent 100-fold drop in potency (comparing compound **4** to compound **3**). Attempts to regain this hydrogen bonding interaction by incorporating an indazolinone failed (compound **5**). The size and length of the pendent 'tail' was important. Increasing the hydrophobicity of these fragments lead to an increase in the biochemical potency, because of increased favorable interactions within the hydrophobic tunnel (compounds **9–11**). If the projection of the hydrophobic tail was away from the tunnel, there was a significant loss in potency (compounds **8** and **12**). Although potent *ee*LpxC inhibitors were synthesized, there was no observed cellular potency with this series of compounds.

The importance of the hydrogen bonding interaction between the peptide amide NH and Thr-179 in terms of biochemical potency and potentially cellular potency lead us to believe that we needed to change our strategy. Instead of a benzolactam fusion we decided upon a urea fusion between the peptide linker and the hydrophobic fragment (Table 2). The synthetic methods used for the preparation of these analogs are illustrated in Scheme 2. The ureas were synthesized by the reaction between the previously prepared hydrophobic fragments and the activated peptide carbamate. The synthesis was then completed with acid hydrolysis and peptide coupling to incorporate the zinc binding hydroxamic acid.

Resolution (1.9 Å) X-ray crystal structures were solved for *aa*LpxC with our urea inhibitors (Fig. 2). These showed the possibility of making key interactions within the active site and hydrophobic tunnel which could aid in the design and synthesis of potent inhibitors. Similar to the benzolactam series of compounds, the projection of this fragment towards the hydrophobic tunnel was a key factor towards maintaining and increasing enzyme potency.

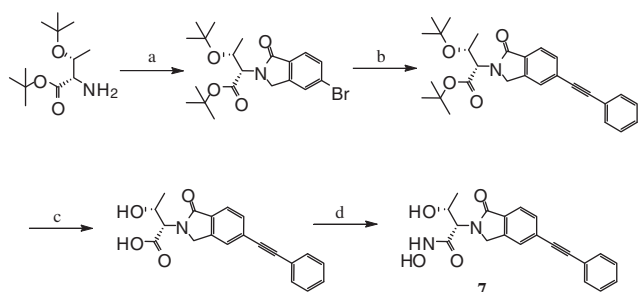
Table 1

SAR of benzolactam series

			<i>ee</i> LpxC IC ₅₀ ^a (nM)
Mol. I.D.	R		
3			2.0
4			130.0
5			200.0
6			>61,000
7			41,000
8			34,000
9			50
10			29
11			13
12			971

^a A high-throughput enzymatic assay using BioTrove Rapid Fire HTS Mass Spectrometry technology was developed for screening.³²

Rigidity of the urea moiety was necessary as shown by the difference in enzyme activity when comparing cyclic ureas to aliphatic



Scheme 1. Reagents and conditions: (a) 4-bromo-2-(bromomethyl)-benzoate, DMF, DIEA, 80 °C, 16 h; (b) dichlorobis-(acetonitrile)palladium (II), X-Phos, cesium carbonate, phenyl acetylene, 90 °C, 2.5 h; (c) TFA, rt, 1 h; (d) *O*-(*tert*-butyldimethylsilyl)hydroxylamine, HATU, DIEA, DMF, rt, 16 h.

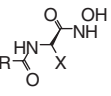
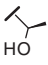
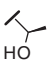
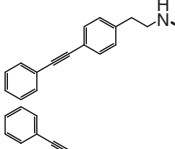
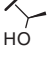
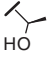
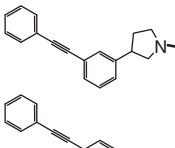
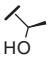
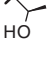
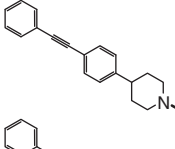
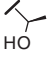
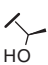
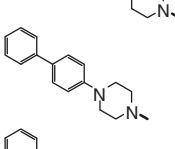
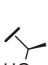
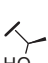
ureas (compounds **13–14** and compound **15**). Ring size (preferably six-membered ring) and connection of the hydrophobic fragment

to the ring (preferably 1,4-connection) also played a role in terms of projection of the 'tail' towards the tunnel (compounds **15–18**). Piperidine or piperazine rings were most optimal. Biochemically these compounds tended to be equipotent, but the piperazine ring generally imparted increased cellular potency, likely due to enhanced polarity, which in turn lead to greater cell penetration (compounds **18** and **19**).

The hydrophobic moiety inserts into the hydrophobic tunnel and depending on the length of the fragment protrudes from the opposite end, similar to TU-514 and fatty acids. Extensive hydrophobic contacts are observed between the inhibitor and residues within the tunnel, including Ile-18, Ala-181, Ile-186, Ile-189, Gly-195, Gly-198, Ser-199, Leu-200 and Thr-203. The aromatic rings of the biphenyl acetylene moiety are not co-planar but are off-set by a -25° dihedral angle. This orientation provides a better fit into the tunnel than simple biaryl fragments, leading to enhanced LpxC enzyme potencies (compounds **18–22**).

Table 2

Enzymatic activity and primary MIC profile of urea series of inhibitors

Mol. I.D.	R	X	<i>ee</i> LpxC IC ₅₀ (nM)			
				<i>ee</i> LpxC MIC ^a HS294 ^b (μg/mL)	<i>ee</i> LpxC MIC ^a ATCC25922 ^c (μg/mL)	<i>pa</i> LpxC MIC ^a ATCC27853 ^c (μg/mL)
3	CHR-12		2.0	0.02	0.08	0.08
13			201.4	12.5	>100	NT ^d
14			1268.9	50	>100	NT
15			36	12.5	100	NT
16			146.4	1.56	100	>100
17			386.7	25	>100	NT
18			2.1	0.8	12.5	6.25
19			2.4	0.2	1.56–3.13	3.13
20			5.6	0.8	3.13	>100
21			13.8	0.8	6.25	3.13

(continued on next page)

Table 2 (continued)

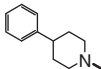
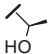
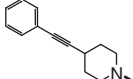
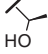
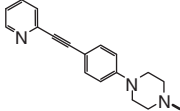
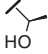
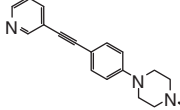
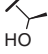
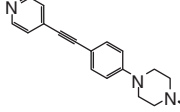
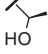
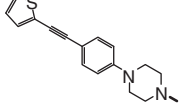
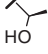
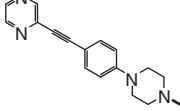
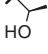
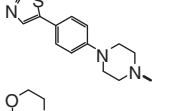
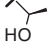
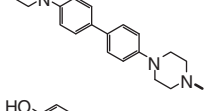
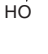
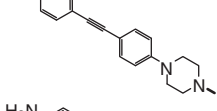
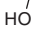
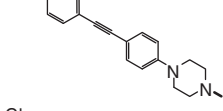
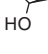
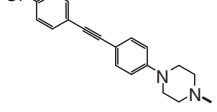
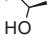
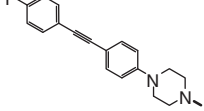
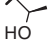
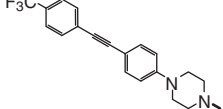
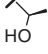
Mol. I.D.	R	X	eeLpxC IC ₅₀ (nM)	eeLpxC MIC ^a HS294 ^b (μg/mL)	eeLpxC MIC ^a ATCC25922 ^c (μg/mL)	paLpxC MIC ^a ATCC27853 ^c (μg/mL)
22			3944.5	12.5	NT	NT
23			207.0	3.13	25	100
24			10	6.25	>100	>100
25			63.0	12.5	100	>100
26			4.0	0.8	3.13	>100
27			21.0	1.56	25	>100
28			136	6.25	>100	>100
29			12.0	3.13	100	>100
30			16.3	3.13	6.25	>100
31			4.0	0.1	1.56	3.13
32			26.0	1.56	3.13	>100
33			5.0	1.56	6.25	>100
34			7.0	0.8	3.13	>100
35			10.4	1.56	12.5	>100

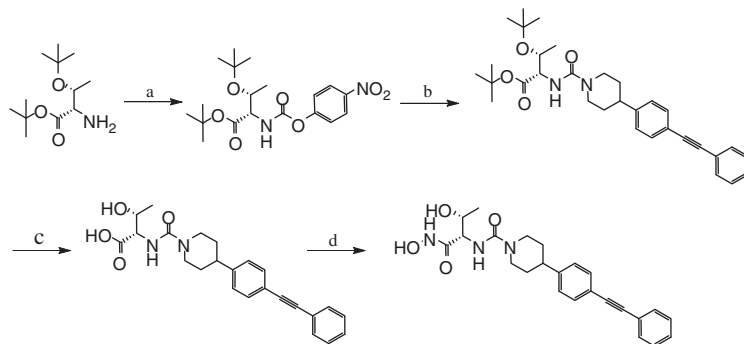
Table 2 (continued)

Mol. I.D.	R	X	eeLpxC IC ₅₀ (nM)	eeLpxC MIC ^a HS294 ^b (μg/mL)	eeLpxC MIC ^a ATCC25922 ^c (μg/mL)	paLpxC MIC ^a ATCC27853 ^c (μg/mL)
36			11.0	0.8	6.25	>100
37			12.0	0.4	12.5	25
38			14.0	1.56	6.25	25
39			3.0	0.1	25	>100
40			23.3	0.4	6.25	6.25
41			0.3	<0.1–0.4	0.8–4	12.5–50
42			2.5	0.2–0.4	0.8–6.25	100
43			7.0	0.8	3.13	>100
44			163.1	6.25	12.5	25
45			0.6	0.4–0.8	1.56–3.13	6.25

^a Minimal inhibitory concentration (MIC) analysis was performed by broth dilution methods according to CLSI standard methods.^b Primary screen included cell wall compromised ('leaky') strains of *E. coli* and *P. aeruginosa*.^c Primary screens also included wild-type strains of *E. coli* and *P. aeruginosa*.^d Not tested.

Not surprisingly removal of a phenyl ring, shortening the hydrophobic fragment (compounds **22** and **23**) results in a drop of potency because of a subsequent loss in the number of key hydrophobic contacts. Introducing polarity to the hydrophobic fragment by replacing the distal phenyl ring with heteroaryls (compounds **24–29**) has a negative impact on potency. This is because the distal ring is still situated in the back end of the hydrophobic tunnel. Only modifications at the 4-position are tolerated (compound **26** and compounds **30–40**). Although the projections of groups at this position are now into the surface of the protein, the main driving force for potency may still be a combination of hydrophobic interactions with the surface of the protein and potential hydrogen bonding interactions with the solvent.

As mentioned earlier, the binding of these inhibitors are further strengthened through interactions with conserved hydrophilic and hydrophobic residues in the active site. We have already described the importance of the hydrogen bond formed by the peptide amide NH and Thr-179 in terms of potency, but there are key interactions which can be targeted to further improve the biochemical potency. The threonine methyl group forms van der Waals contacts with the aromatic ring of Phe-180, while the threonine hydroxyl group is well positioned to form hydrogen bonds with Lys-227, Aps-230 and the positively charged His-253 imidazole group. It is therefore not surprising that modifications at this position have a tremendous impact on enzyme potency. Replacing the threonine motif with a *gem*-dimethyl hydroxyl group (compounds **41–43**) leads



Scheme 2. Reagents and conditions: (a) 4-nitrophenyl chloroformate, DIEA, THF, 0 °C, 1 h; (b) R_2NH , DIEA, THF, 80 °C, 2 h; (c) TFA, rt, 1 h; (d) *O*-(*tert*-butyldimethylsilyl)hydroxylamine, HATU, DIEA, DMF, rt, 16 h.

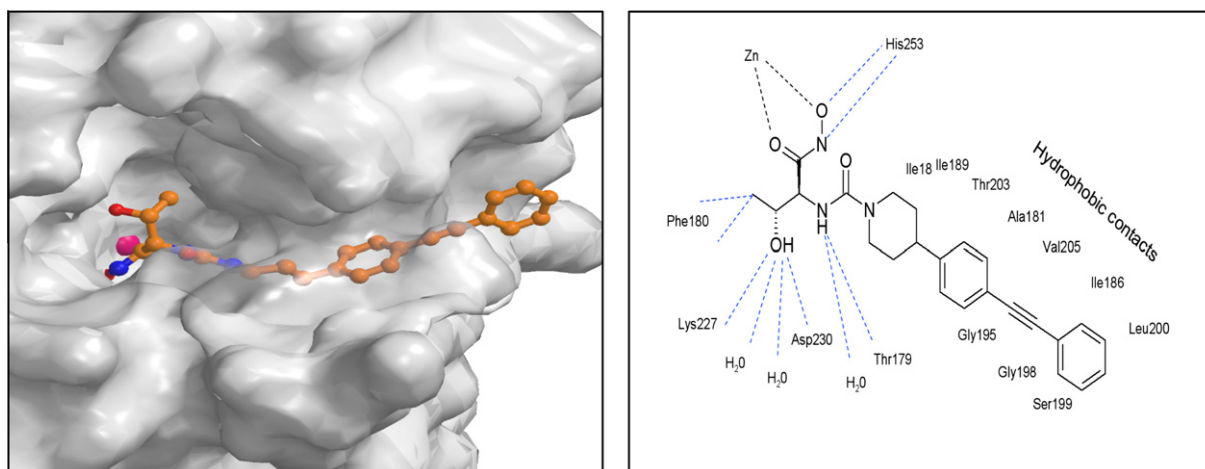


Figure 2. X-ray structure solved for *aALPxC* with compound **18** at 1.9 Å.³³ Molecular interaction map detailing key polar and non-polar interactions within the *aALPxC* active site and hydrophobic tunnel.

Table 3

Expanded Gram-negative MIC (μg/mL) profile for LpxC inhibitors

Organism	Resistance Phenotype	Compound 21	Compound 41	Compound 45	Compound 3 (CHR-12)	Ciprofloxacin	Tetracycline	Chloramphenicol	Ampicillin	Azithromycin
<i>E. coli</i>	Wild-type	1.56	0.8	1.56	0.16	0.008	1	2	4	
<i>E. coli</i>	MDR	3.13	3.13	3.13	0.63	>32	2	>256	>256	64
<i>E. coli</i>	MDR	3.13	1.56	3.13	0.63	>32	>256	32	8	32
<i>E. coli</i>	ESBL	3.13	1.56	1.56	0.313	0.016			>32	
<i>E. coli</i>	ESBL	3.13	3.13	3.13	0.63					
<i>E. coli</i>	Wild-type	6.25	12.5	3.13	1.25					
<i>P. aeruginosa</i>	Wild-type	3.13	>50	12.5	10	0.012	1	2	4	4
<i>P. aeruginosa</i>	MDR	>100	12.5	12.5	2.5	>32	16	>256	>256	32
<i>P. aeruginosa</i>	MDR	12.5	6.25	3.13	0.63	8	64	>256	>256	
<i>S. maltophilia</i>	Wild-type	>100	25	>50	5	0.016			>32	
<i>K. pneumoniae</i>	Wild-type	>100	12.5	25	1.25	1			>32	
<i>K. pneumoniae</i>	ESBL	12.5	6.25	12.5	0.63				>32	
<i>P. vulgaris</i>	Wild-type	3.13	3.13	6.25	1.25					
<i>S. marcescens</i>	Wild-type	6.25	6.25	12.5	1.25					
<i>E. aerogenes</i>	Wild-type	>100	12.5	25	2.5					
<i>E. cloacae</i>	ESBL	3.13	6.25	3.13	0.31				>32	
<i>A. calcoaceticus</i>	Wild-type	>100	25	25	1.25					
<i>A. anitratus</i>	Wild-type	>100	25	25	1.25					
<i>A. baumannii</i>	Wild-type	>100	>50	25	>20					

to an almost 10-fold increase in potency. Likewise, removal of the potential for van der Waals interactions leads to a significant drop in activity (compound **44**).

We have demonstrated that enzyme potency can be achieved by exploiting several conserved and essential features of LpxC to

form a tight-binding complex (catalytic zinc binding, binding of the peptide linker, and maintaining hydrophobic contacts within the hydrophobic tunnel). However, achieving cellular potency requires finding the right balance between polarity and hydrophobicity as shown by compound **45**.

Some of the compounds which showed good activity against wild-type *E. coli* and *P. aeruginosa* were screened for anti-microbial activity against resistant and expanded spectrum Gram-negative pathogens (Table 3). The results show that a number of Gram-negative selective compounds have been identified which are potent LpxC inhibitors with good whole-cell activities and spectrum anti-bacterial properties.

In conclusion, we have designed two series of novel benzolactam and urea derivatives which have potent LpxC inhibitor activity. The results illustrate that enzyme activity is determined by a number of factors including coordination of the zinc-binding motif, hydrophilic and hydrophobic interactions within the active site, and key hydrophobic contacts inside the hydrophobic tunnel. Efforts are currently underway to solve X-ray crystal structures for *P. aeruginosa* with our inhibitors which will aid future drug design of potent LpxC inhibitors.

References and notes

- Levy, S. B. *Adv. Drug Delivery Rev.* **2005**, *57*, 1446.
- Levy, S. B.; Marshall, B. *Nat. Med.* **2004**, *10*, S122.
- Walsh, C. T. *Nat. Rev. Microbiol.* **2003**, *1*, 65.
- Projan, S. J. *Curr. Opin. Pharmacol.* **2002**, *2*, 513.
- Raetz, C. R. H. *Annu. Rev. Genet.* **1986**, *20*, 253.
- Gronow, S.; Brade, H. J. *Endotoxin Res.* **2001**, *7*, 3.
- Raetz, C. R. H.; Whitfield, C. *Annu. Rev. Biochem.* **2002**, *71*, 635.
- Raetz, C. R. H. *J. Bacteriol.* **1993**, *175*, 5745.
- Wyckoff, T. J. O.; Raetz, C. R. H.; Jackman, J. E. *Trends Microbiol.* **1998**, *6*, 154.
- Nikaido, H.; Vaara, M. *Microbiol. Rev.* **1985**, *49*, 1.
- Vaara, M. *Antimicrob. Agents Chemother.* **1993**, *37*, 354.
- Vuorio, R.; Vaara, M. *Antimicrob. Agents Chemother.* **1992**, *36*, 826.
- Onishi, H. R.; Pelak, B. A.; Gerckens, L. S.; Silver, L. L.; Kahan, F. M.; Chen, M.-H.; Patchett, A. A.; Galloway, S. M.; Hyland, S. A.; Anderson, M. S.; Raetz, C. R. H. *Science* **1996**, *274*, 980.
- Kline, T.; Andersen, N. H.; Harwood, E. A.; Bowman, J.; Malanda, A.; Endsley, S.; Erwin, A. L.; Doyle, M.; Fong, S.; Harris, A. L.; Mendelsohn, B.; Mdluli, K.; Raetz, C. R. H.; Stover, C. K.; Witte, P. R.; Yabannavar, A.; Zhu, S. J. *Med. Chem.* **2002**, *45*, 3112.
- Clements, J. M.; Coignard, F.; Johnson, I.; Chandler, S.; Palan, S.; Waller, A.; Wijkman, J.; Hunter, M. G. *Antimicrob. Agents Chemother.* **2002**, *46*, 1793.
- Pirrung, M. C.; Tumey, L. N.; Raetz, C. R. H.; Jackman, J. E.; Snehalatha, K.; McClerren, A. L.; Fierke, C. A.; Gantt, S. L.; Rusche, K. M. *J. Med. Chem.* **2002**, *45*, 4359.
- Anderson, M. S.; Bulawa, C. E.; Raetz, C. R. H. *J. Biol. Chem.* **1985**, *260*, 15536.
- Anderson, M. S.; Robertson, A. D.; Macher, I.; Raetz, C. R. H. *Biochemistry* **1988**, *27*, 1908.
- Anderson, M. S.; Bull, H. G.; Galloway, S. M.; Kelly, T. M.; Mohan, S.; Radika, K.; Raetz, C. R. H. *J. Biol. Chem.* **1993**, *268*, 19858.
- Young, K.; Silver, L. L.; Bramhill, D.; Cameron, P.; Eveland, S. S.; Raetz, C. R. H.; Hyland, S. A.; Anderson, M. S. *J. Biol. Chem.* **1995**, *270*, 30384.
- Hernick, M.; Fierke, C. A. *Arch. Biochem. Biophys.* **2005**, *433*, 71.
- Hernick, M.; Gennadios, H. A.; Whittington, D. A.; Rusche, K. M.; Christianson, D. W.; Fierke, C. A. *J. Biol. Chem.* **2005**, *280*, 16969.
- McClerren, A. L.; Zhou, P.; Guan, Z.; Raetz, C. R. H.; Rudolph, J. *Biochemistry* **2005**, *44*, 1106.
- Whittington, D. A.; Rusche, K.; Shin, H.; Fierke, C. A.; Christianson, D. W. *Proc. Natl. Acad. Sci. U.S.A.* **2003**, *100*, 8146.
- Jackman, J. E.; Raetz, C. R. H.; Fierke, C. A. *Biochemistry* **1999**, *38*, 1902.
- Jackman, J. E.; Fierke, C. A.; Tumey, L. N.; Pirrung, M.; Uchiyama, T.; Tahir, S. H.; Hindsgaul, O.; Raetz, C. R. H. *J. Biol. Chem.* **2000**, *275*, 11002.
- Li, X.; Uchiyama, T.; Raetz, C. R. H.; Hindsgaul, O. *Org. Lett.* **2003**, *5*, 539.
- Coggins, B. E.; Li, X.; McClerren, A. L.; Hindsgaul, O.; Raetz, C. R. H.; Zhou, P. *Nat. Struct. Biol.* **2003**, *10*, 645.
- Coggins, B. E.; McClerren, A. L.; Jiang, L.; Li, X.; Rudolph, J.; Hindsgaul, O.; Raetz, C. R. H.; Zhou, P. *Biochemistry* **2005**, *44*, 1114.
- Gennadios, H. A.; Whittington, D. A.; Li, X.; Fierke, C. A.; Christianson, D. W. *Biochemistry* **2006**, *45*, 7940.
- Shin, H.; Gennadios, H. A.; Whittington, D. A.; Christianson, D. W. *Bioorg. Med. Chem.* **2007**, *15*, 2617.
- Ozbal, C. C.; LaMarr, W. A.; Linton, J. R.; Green, D. F.; Katz, A.; Morrison, T. B.; Brenan, C. J. *Assay Drug Dev. Technol.* **2004**, *2*, 373.
- X-ray crystal structure (PDB ID code 3P76) deposited with the RCSB protein data bank (PDB).